Stem Cell Reports, Volume *8*

Supplemental Information

Long-Term Adult Feline Liver Organoid Cultures for Disease Modeling of Hepatic Steatosis

Hedwig S. Kruitwagen, Loes A. Oosterhoff, Ingrid G.W.H. Vernooij, Ingrid M. Schrall, Monique E. van Wolferen, Farah Bannink, Camille Roesch, Lisa van Uden, Martijn R. Molenaar, J. Bernd Helms, Guy C.M. Grinwis, Monique M.A. Verstegen, Luc J.W. van der Laan, Meritxell Huch, Niels Geijsen, Robert G. Vries, Hans Clevers, Jan Rothuizen, Baukje A. Schotanus, Louis C. Penning, and Bart Spee

Figure S1. Performance of different expansion media in short and long-term feline liver organoid culture. Related to Figure 1 and Experimental Procedures.

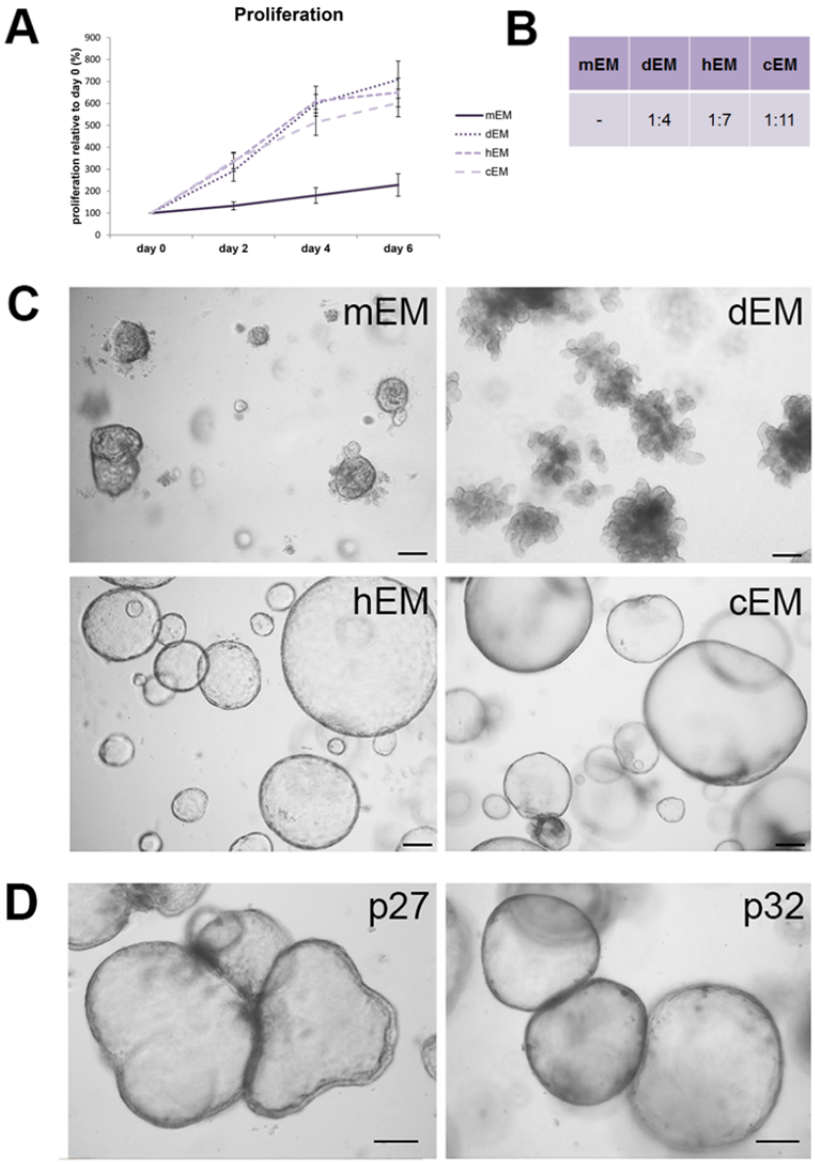

Figure S1. Performance of different expansion media in short and long-term feline liver organoid culture. Related to Figure 1 and Experimental Procedures.

(A) Short term proliferation as indicated by an Alamar blue growth curve of feline liver organoids cultured in mouse, dog, human and cat expansion medium (mEM, dEM, hEM, and cEM, respectively). Organoids showed significantly less proliferation on mEM than on the other expansion media within one week of culturing. n=4 donors per culture condition. Error bars indicate standard deviation.

(B) Long term expansion potential of feline liver organoids cultured in mEM, dEM, hEM, and cEM as indicated by weekly split rates from passage 11 to passage 26. Mouse EM failed to support feline liver organoid growth for more than five passages for two donors, with a maximum of 15 passages for other donors.

(C) Representative phase contrast images of feline liver organoids cultured in mEM, dEM, hEM, and cEM. In mEM feline organoids remained small and were surrounded by cellular debris. Feline organoids cultured in dEM were heavily folded, and had a round appearance in hEM and cEM. cEM performed best and allowed for a high split ratio (1:11) in long-term culture. Scalebars represent 100 µm.

(D) Representative phase contrast images of feline liver organoids in cEM in long-term culture. Growth slowed down after passage 27 (p27) but cultures could be continuously expanded until at least passage 32 (p32). Scalebars represent 100 µm.

Figure S2. Flow cytometry analysis of LD540 in liver organoids. Related to Figure 4.

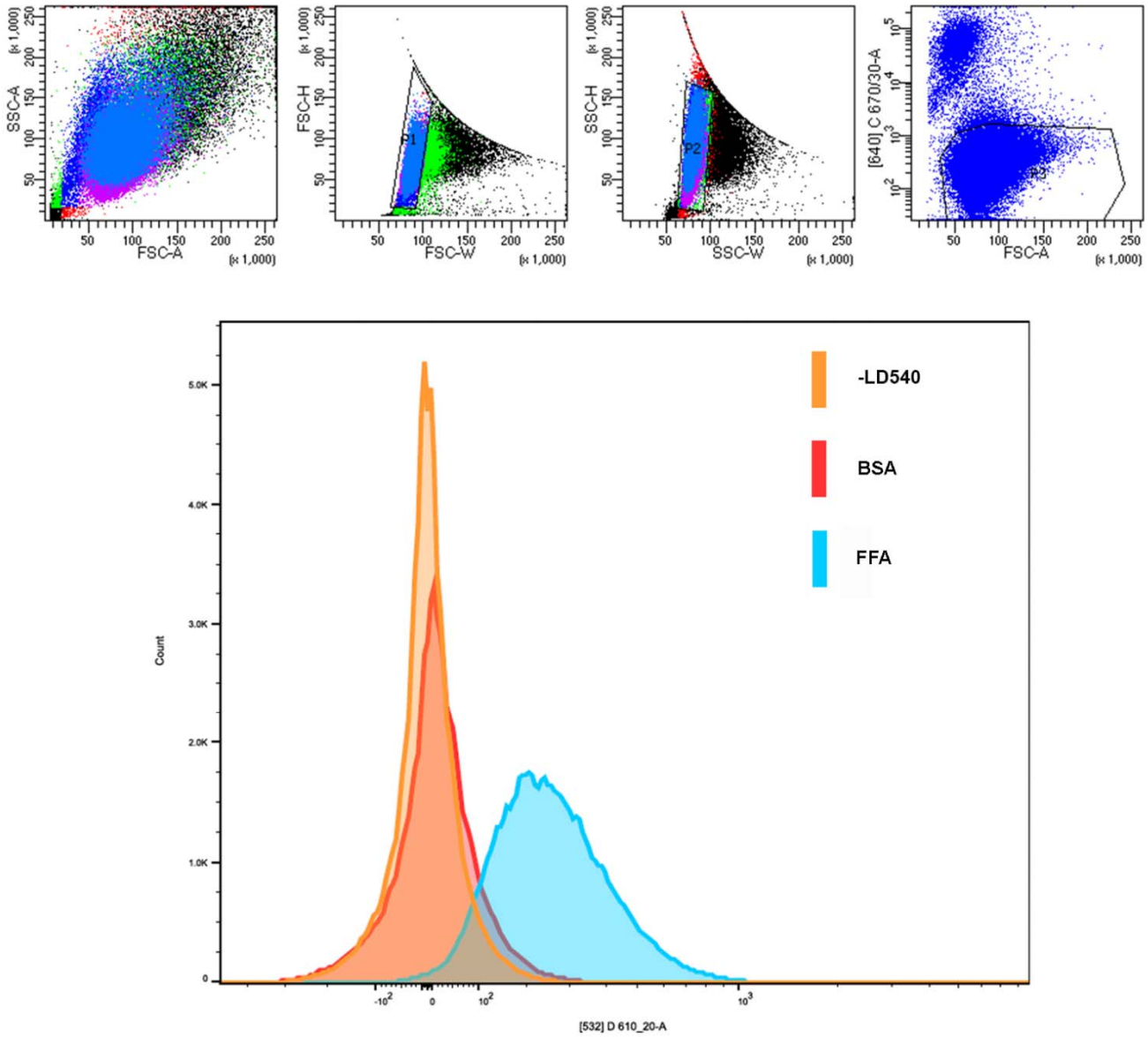

Figure S2. Flow cytometry analysis of LD540 in liver organoids. Related to Figure 4.
Representative plots are shown of a liver organoid flow cytometry experiment to illustrate workflow and data analysis. Single cells were selected in gate P1 and P2 based on forward scatter (FSC) and side scatter (SSC). Next, live cells were selected in gate P3 based on Sytox red exclusion (670/30 emission). To detect lipid accumulation in cells using LD540 a 532 nm laser with emission detection at 610/20 nm was used. LD540 median fluorescence intensity of the population was calculated and compared between cells treated with BSA (control) and cells treated with free fatty acids (FFA). Cells treated with FFA but not stained with LD540 served as a technical negative control to rule out autofluorescence.

Figure S3. Gene expression analysis of human and feline liver organoids after treatment with free fatty acids. Related to Figure 4.

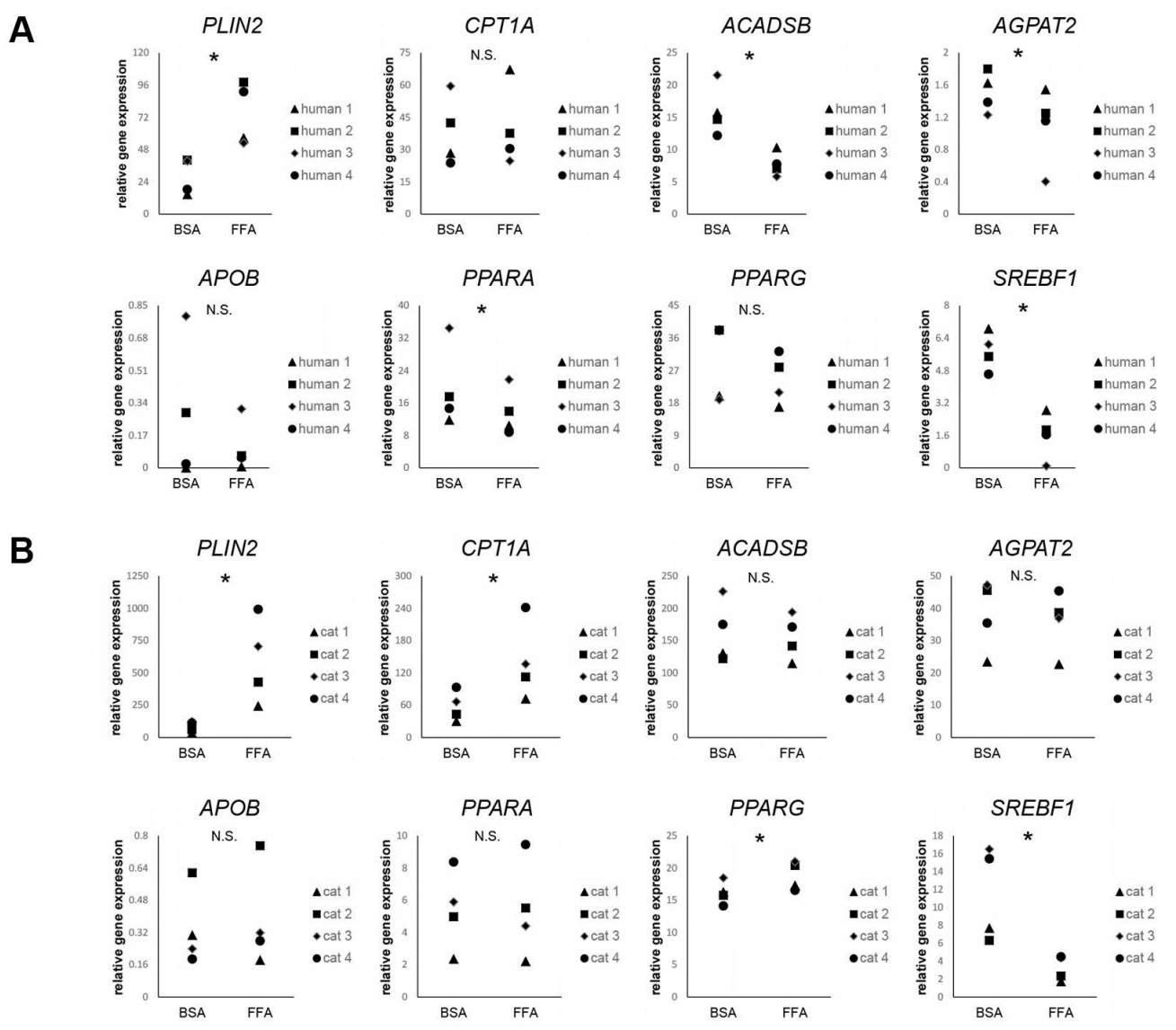

Figure S3. Gene expression analysis of human and feline liver organoids after treatment with free fatty acids. Related to Figure 4.

(A) Relative gene expression of human liver organoids treated with free fatty acids (FFA) compared to control treatment (BSA). n=4 donors per experimental condition. N.S.: not significant; * indicates significance ($p<0.05$, Wilcoxon signed rank test).

(B) Relative gene expression of feline liver organoids treated with free fatty acids (FFA) compared to control treatment (BSA). n=4 donors per experimental condition. N.S.: not significant; * indicates significance ($p<0.05$, Wilcoxon signed rank test).

Supplemental Experimental Procedures

Liver samples

Surplus liver samples (wedge biopsies of 5 mm^3) were obtained postmortem from five cats. From one cat, both a wedge biopsy and a fine needle aspirate (FNA, 22G) from the liver were taken. Liver was sampled fresh and processed immediately or frozen in freezing medium (Gibco). Three out of five samples originated from a frozen biobank, were snap frozen upon sampling and had been stored for seven years at -70°C prior to use in this study (surplus material of cats used in non-liver related research, approved by the Utrecht University's ethical committee as required under Dutch legislation).

RNA isolation, cDNA synthesis and quantitative reverse transcription PCR

RNA from organoids (n=4 donors per species) and normal cat liver (n=3 donors) was isolated and converted to cDNA as described previously (Nantasanti et al., 2015). QPCR was performed in duplicate on three culture replicates per donor on a BioRad MyiQ thermal cycler using SYBRgreen supermix (BioRad). Species specific primers were developed for leucine-rich repeat-containing G protein-coupled receptor 5 (*LGR5*); prominin 1/CD133 (*PROM1*); B cell-specific Moloney murine leukaemia virus integration site 1 (*BMI1*); keratin 7 (*KRT7*); keratin 19 (*KRT19*); hepatic nuclear factor 1 homeobox β (*HNF1β*); hepatic nuclear factor 4 homeobox α (*HNF4α*); T-box 3 (*TBX3*); albumin (*ALB*); prospero homeobox 1 (*PROX1*); pyruvate carboxylase (*PC*); 3-hydroxymethyl-3-methylglutaryl-CoA lyase (*HMGCL*); transthyretin (*TTR*); fumarylacetoacetate hydrolase (*FAH*); cytochrome 3A132 (*CYP3A132*); perilipin 2 (*PLIN2*); carnitine palmitoyltransferase 1A (*CPT1A*); acyl-CoA dehydrogenase, short/branched chain (*ACADSB*); 1-acylglycerol-3-phosphate O-acyltransferase 2 (*AGPAT2*); apolipoprotein B (*APOB*); peroxisome proliferator activated receptor alpha (*PPARA*); peroxisome proliferator activated receptor gamma (*PPARG*); and sterol regulatory element binding transcription factor 1 (*SREBF1*) (lipid metabolism genes were derived from Wruck et al., 2015, and Graffmann et al., 2016). For feline cells, tyrosine 3-monooxygenase/ tryptophan 5-monooxygenase activation protein, zeta (*YWHAZ*), ribosomal protein S5 (*RPS5*) and hypoxanthine phosphoribosyltransferase (*HPRT-1*) were used as reference genes to calculate relative gene expression (delta Cq method). For human cells beta-2-microglobulin (*B2M*), *HPRT-1* and ribosomal protein L19 (*RPL19*) were used as reference genes. Expression levels that were undetectable were arbitrarily set to a Cq value of 45. Primer details are listed in Table S1.

Immunocyto-/histochemical and whole mount immunofluorescent staining

Organoids were fixed in 10% neutral buffered formalin, embedded in paraffin and sections of 4 µm were cut. H&E staining was routinely performed. For immunocyto-/histochemical staining of K19, HNF1β, BMI1, albumin, HepPar-1, and tight junction protein 1 (ZO1), sections were dewaxed and rehydrated and antigen retrieval was performed (methods listed in Table S2). Sections were blocked with 10% normal goat serum (NGS, Sigma-Aldrich) and primary antibody was incubated at 4°C overnight (antibody dilutions listed in Table S2). As negative control, isotype antibodies were used or primary antibody was omitted. Secondary antibody was incubated for 45 minutes at room temperature (EnVision, Dako), signal was visualized with 3,3'-diaminobenzidine and sections were counterstained with haematoxylin. Imaging was performed using an Olympus microscope (CKX41) in combination with a Leica DFC425C camera. PAS staining was performed routinely.

For whole mount immunofluorescent staining feline liver organoids were carefully harvested from Matrigel and fixed in 10% neutral buffered formalin for 45 minutes on ice. Organoids were permeabilized and blocked with 0.5% v/v Triton X100, 1% v/v DMSO, 1% w/v BSA, and 10% v/v NGS in PBS. Mouse anti-E-cadherin (BD Biosciences) was diluted 1:500 and incubated at 4°C over two nights. Secondary goat anti-mouse AF488 antibody (Life Technologies) was diluted 1:100 and incubated for 2 hours at room temperature. Nuclei were stained with 4',6-Diamidine-2'-phenylindole (DAPI, Sigma-Aldrich). Organoids were mounted using ProLong Diamond Antifade mounting medium (Life Technologies) and imaged using a confocal microscope (Leica). An EdU incorporation assay and whole mount imaging was performed as described previously (Nantasanti et al., 2015). Briefly, organoids in log-phase of growth were pulsed with 10 µM 5-ethynyl-2´-deoxyuridine (EdU, thymidine analogue) for six hours, fixed and stained with 5 µM AF488 azide, 100 mM ascorbic acid, and 1mM $CuSO_4$ in a click reaction. Nuclei were stained with DAPI. For LD540 whole mount staining, fixed organoids were incubated in 0.025 µg/mL LD450 in PBS for 1 hour at room temperature. After washing, nuclei were stained with DAPI and organoids were mounted with ProLong Diamond Antifade mounting medium (Life Technologies) and imaged using a confocal microscope (Leica).

Karyotyping

Feline liver organoids of four donors in low (p3-7) and high (p16-23) passage numbers in log-phase of growth were arrested in metaphase with 15 µg/ml colchicine (KaryoMax, Gibco) overnight. Organoids were trypsinized to single cell level, incubated with hypotonic buffer (0.075 M KCl) for 10 minutes and then fixed

with methanol-acetic acid (3:1). Chromosome spreads were routinely prepared and imaged using an Olympus fluorescence microscope. At least 100 spreads were counted for both low and high passages numbers; a chromosome count of n=38 is normal for feline cells.

Hepatic function tests after feline liver organoid differentiation

Feline liver organoids of four donors were incubated with DM for seven days. DM was replaced every other day. As control, culture was continued in parallel with EM for all four donors until day 7. Proliferation was measured on days 0, 2, 4, and 7 of differentiation with an Alamar blue assay according to the manufacturer's instructions (Life Technologies). Wells were washed and organoid culture was continued with EM/DM, allowing for serial measurements on the same wells throughout the experiment (growth curve). On day 7, medium was harvested for albumin measurement and organoids were harvested for immunocytochemistry, gene expression analysis, liver enzyme measurement, and CYP450 assay (n=3 wells per donor). Albumin detection in the medium and liver-specific enzyme aspartate aminotransferase (AST) detection in organoid lysates were performed as described previously (Nantasanti et al., 2015). Cytochrome P450 activity was measured according to the manufacturer's instructions with the P450-Glo™ assay (Promega) specific for CYP3A4. CYP3A is one of the major cytochromes active in feline liver (Van Beusekom et al., 2010). All values were corrected for cell input with Alamar blue.

Fatty acid treatment of liver organoids

Liver organoids in similar passage number (p5-7) of mouse, human, dog and cat were cultured in 12 well plates in their specific EM for three days (four donors per species). For free fatty acid (FFA) treatment, a generic organoid expansion medium was designed for all species to accommodate for differences in lipid content of the medium (*e.g.* dog EM contains serum), which consisted of Advanced DMEM/F12, supplemented with 1% v/v penicillin-streptomycin, 1% v/v GlutaMax, 10 mM Hepes (all Gibco), 2% v/v B27 minus vitamin A (Invitrogen), 1% v/v N2 (Invitrogen), 10 mM nicotinamide (Sigma-Aldrich), 1.25 mM N-acetylcysteine (Sigma-Aldrich), 5% v/v R-spondin-1 conditioned medium, 25 ng/ml HGF (Peprotech), 0.1 µg/ml FGF10 (Peprotech), and 10 nM gastrin (Sigma-Aldrich). Either 0.4 mM oleate (C18:1) and 0.2 mM palmitate (C16:0) coupled to 12% w/v fatty acid-free BSA were added (all from Sigma-Aldrich) or only fatty acid-free BSA as vehicle control. FFA concentrations were based on pilot experiments (data not shown) and literature (Gómez-Lechón et al., 2007). Organoids were cultured with either free fatty acids (FFA) or BSA for 24 hours and were then harvested for RNA isolation, whole mount staining with LD540 and flow cytometry.

For feline organoids the β oxidation of excess FFA was studied by culturing them with either fatty acid-free BSA (control), FFA (0.4 mM oleate and 0.2 mM palmitate), FFA plus 50 µM etomoxir (carnitine palmitoyltransferase-1 inhibitor, Cayman), or FFA plus 1 mM L-carnitine (Selleckchem). DMSO was used as solvent for etomoxir and was therefore added as vehicle control to the other treatment media. Concentration of etomoxir was based on pilot experiments (data not shown); concentration of L-carnitine was based on literature (Odle et al., 1995). Pictures before and after 24 hours of treatment were taken with a Olympus microscope in combination with a Leica camera. Feline liver organoids were then harvested for flow cytometry.

Statistical tests

Data are presented as mean ± SD. Statistical analysis was performed in SPSS (IBM SPSS Statistics 22). All statistical tests were performed on four biological replicates. A Kruskall Wallis test was performed in cases of multiple group testing. A nonparametric Mann Whitney U test was performed on independent samples. A nonparametric 1-tailed Wilcoxon signed rank test was used for related samples. $P<0.05$ was considered significant.

Table S1. Primer sequences and QPCR conditions

Species	Gene	Direction	Sequence (5' – 3')	Tm (°C)	Product size (bp)
Cat	*LGR5*	Forward	GGAAAGTTTGACTTTAACTGGA	58	101
		Reverse	GCAGGTTGTAAGATAGATCTAGCA		
	PROM1	Forward	TGAGCCAGTACACCACCA	61	150
		Reverse	GTCTCTTTGATTGCTTCTGCC		
	BMI1	Forward	CAATGGCTCTAACGAAGATAGAG	60	120
		Reverse	TACTTTCCGATCCAATCTGTTCTG		
	KRT7	Forward	CCAGACCAAGTTTGAGACC	58	131
		Reverse	TCTTAATGCTGTCGATCTCAG		
	KRT19	Forward	AATCACGAGGAGGAAGTCAG	58	106

		Reverse	CGTCACTCAGGATCTTGG		
	HNF1β	Forward	GTCACAGGTCTGAACCAG	61	130
		Reverse	GGTTGAATTGTCGGAGGA		
	HNF4α	Forward	TGTACTCCTGCAGATTTAGTC	58	88
		Reverse	CGGAAGCACTTCTTGAGC		
	TBX3	Forward	GAAGAAGAGGTGGAGGATGAC	63	115
		Reverse	GAAACATTCGCCTTCCCG		
	ALB	Forward	CGAGAAGCACATCAGAGTG	58	84
		Reverse	AAAGGCAACCAGTACCAG		
	PROX1	Forward	GCAGGAAGGATTGTCACC	58	118
		Reverse	GCATCTGTTGAACTTTACATCG		
	PC	Forward	TCAATACCCGCCTCTTCC	61	109
		Reverse	GTTCAGGTCACTTATAGCCAG		
	HMGCL	Forward	GGGCATCAGGAAACTTGG	65	83
		Reverse	GCTTCTGGAGGTTCACAC		
	TTR	Forward	CAAAGTGGAAATAGACACCAAGTC	58	81
		Reverse	GTGAACACCACCTCTGCA		
	FAH	Forward	GAGTCCTTGCGGAATCTG	58	129
		Reverse	CGTGTAGTCACCTATGGC		
	CYP3A132	Forward	GGTGCTCCTCTATCTATATGGGA	60	201
		Reverse	TCTGTGATCGCCAACACTG		
	PLIN2	Forward	TCGCAGTTAATCCACAACC	64	127
		Reverse	CACGGACTTCAAGCAAGG		
	CPT1A	Forward	CCGAACATTCCGTATCCCA	63	150
		Reverse	TGATGAGTCCTTTGCCGA		
	ACADSB	Forward	TTTGCCCAGGAACAGATTGC	62	109
		Reverse	TTTCAATACCCATCAACCCTTGC		
	AGPAT2	Forward	GTCTTCTTCATCAACCGGCAG	61	95
		Reverse	ACCCACACCTTGAGATTCTCC		
	APOB	Forward	ACTCGATTCAAGCACCTCC	66	123
		Reverse	GCACCTCCAGTTCAACCT		
	PPARA	Forward	GACAAATGTGACCGTAGCTG	60	109
		Reverse	AAACGAATTGCGTTATGGGA		
	PPARG	Forward	TGTGACCTTAACTGTCGTATCC	66	134
		Reverse	CTTCTCTTTCTCCGCCTGTG		
	SREBF1	Forward	CGTTTCTTCGTGGATGGG	63	140
		Reverse	ACAATTCAGTGCTCGCTC		
	YWHAZ	Forward	GAAGAGTCCTACAAAGACAGCACGC	65	115
		Reverse	AATTTTCCCCTCCTTCTCCTGC		
	RPS5	Forward	CAGGTCTTGGTGAATGCG	58	129
		Reverse	CCAGATGGCCTGATTCAC		
	HPRT-1	Forward	TTATGGACAGGACCGAGC	60	107
		Reverse	GTCAGCAAAGAATTTATAGCCC		
Human	*PLIN2*	Forward	GCTGAGCACATTGAGTCACG	58	102
		Reverse	TGGTACACCTTGGATGTTGG		
	CPT1A	Forward	CCTACCACGGGTGGATGTTC	61	101
		Reverse	CAACATGGGTTTTCGGCCTG		
	ACADSB	Forward	CACCATTGCAAAGCATATCG	65	117
		Reverse	GCAAGGCACTTACTCCCAAC		
	AGPAT2	Forward	CCGAGTTCTACGCCAAGGTC	61	121
		Reverse	CCGATGATGCTCATGTTCTCC		
	APOB	Forward	ATCTTCAACATGGCGAGGGA	61	81
		Reverse	TGTCTTATGATAGTTGTTGACCGC		
	PPARA	Forward	AACATCCAAGAGATTTCGCAATCC	60	121
		Reverse	AAAGCGTGTCCGTGATGACC		
	PPARG	Forward	GATGTCTCATAATGCCATCAGGT	65	108
		Reverse	TCAGCGGACTCTGGATTCAG		
	SREBF1	Forward	CCAGGTGACTCAGCTATTCC	61	110

		Reverse	CATCCGAGAATTCCTTGTCCC		
	B2M	Forward	CTTTGTCACAGCCCAAGATAG	58	83
		Reverse	CAATCCAAATGCGGCATCTTC		
	HPRT-1	Forward	TATTGTAATGACCAGTCAACAG	60	192
		Reverse	GGTCCTTTTCACCAGCAAG		
	RPL19	Forward	ATGAGTATGCTCAGGCTTCAG	64	150
		Reverse	GATCAGCCCATCTTTGATGAG		

Table S2. Antibody specifications and antigen retrieval methods

Antibody	**Source**	**Clone**	**Company**	**Dilution**	**Antigen retrieval**
K19	mouse	b170	Novocastra	1:300	10 mM citrate pH 6.0 98°C
HNF1β	rabbit		Sigma	1:400	10 mM citrate pH 6.0 98°C
BMI1	mouse	F6	Millipore	1:300	10mM Tris 1mM EDTA pH 9.0 98°C
albumin	mouse	HSA-11	Sigma	1:2500	10mM Tris 1mM EDTA pH 9.0 98°C
HepPar-1	mouse	OCH1E5	Dako	1:50	10mM Tris 1mM EDTA pH 9.0 98°C
ZO1	rabbit		Invitrogen	1:250	0.8% pepsin 37°C

Supplemental References

Van Beusekom, C.D., Schipper, L., and Fink-Gremmels, J. (2010). Cytochrome P450-mediated hepatic metabolism of new fluorescent substrates in cats and dogs. J. Vet. Pharmacol. Ther. *33*, 519-527.

Gómez-Lechón, M.J., Donato, M.T., Martínez-Romero, A., Jiménez, N., Castell, J.V., and O'Connor J.E. (2007). A human hepatocellular in vitro model to investigate steatosis. Chem. Biol. Interact. *165*, 106-116.

Graffmann, N., Ring, S., Kawala, M.A., Wruck, W., Ncube, A., Trompeter, H.I., and Adjaye J. (2016). Modeling Nonalcoholic Fatty Liver Disease with Human Pluripotent Stem Cell-Derived Immature Hepatocyte-Like Cells Reveals Activation of PLIN2 and Confirms Regulatory Functions of Peroxisome Proliferator-Activated Receptor Alpha. Stem Cells Dev. *25*, 1119-33.

Nantasanti, S., Spee, B., Kruitwagen, H.S., Chen, C., Geijsen, N., Oosterhoff, L.A., Van Wolferen, M.E., Pelaez, N., Fieten, H., Wubbolts, R.W., et al. (2015). Disease modeling and gene therapy of copper storage disease in canine hepatic organoids. Stem Cell Reports *5*, 895-907.

Odle, J., Lin, X., Van Kempen, T.A., Drackley, J.K., and Adams, S.H. (1995). Carnitine palmitoyltransferase modulation of hepatic fatty acid metabolism and radio-HPLC evidence for low ketogenesis in neonatal pigs. J. Nutr. *125*, 2541-2549.

Wruck, W., Kashofer, K., Rehman, S., Daskalaki, A., Berg, D., Gralka, E., Jozefczuk, J., Drews, K., Pandey, V., Regenbrecht, C., et al. (2015). Multi-omic profiles of human non-alcoholic fatty liver disease tissue highlight heterogenic phenotypes. Sci Data *2*, 150068.